

AD-A251 517



2

OFFICE OF NAVAL RESEARCH

Contract No. N00014-91-J-1409

Technical Report No. 129

Iodine Adlayer Structures on Au(111) as Discerned by  
Atomic-Resolution Scanning Tunneling Microscopy:  
Relation to Iodide Electrochemical Adsorption

by

W. Haiss, J.K. Sass, X. Gao, and M.J. Weaver

Prepared for Publication

in

Surface Science

Fritz-Haber Institut der Max-Planck-Gesellschaft

Faradayweg 4-6

D-1000 Berlin 33, Germany

May 1992

DTIC  
ELECTE  
JUN 08 1992  
S B D

Reproduction in whole, or in part, is permitted for any purpose of the United States Government.

\* This document has been approved for public release and sale: its distribution is unlimited.

92-14933



92 6 05 057

**Iodine Adlayer Structures on Au(111) as Discerned  
by Atomic-Resolution Scanning Tunneling Microscopy:  
Relation to Iodide Electrochemical Adsorption**

W. Haiss, J. K. Sass, X. Gao\*, and M. J. Weaver#

*Fritz-Haber-Institut der Max-Planck-Gesellschaft  
Faradayweg 4-6, D-1000 Berlin 33, Germany*

**Abstract**

Coverage-dependent adlayer structures of iodine on Au(111) in air or organic solvents are reported in comparison with those obtained under potential control in aqueous electrochemical environments by means of atomic-resolution scanning tunnelling microscopy (STM). The well-known ( $\sqrt{3} \times \sqrt{3}$ ) R30° structure ( $\Theta_I = 0.33$ ) was only observed at the electrochemical interface at low potentials. Two higher coverage adlattices were evident from the STM images. The first comprises a ( $5 \times \sqrt{3}$ ) structure ( $\Theta_I = 0.40$ ), with a pair of iodine rows compressed by 20 % in the R30° substrate direction. The second high-coverage phase ( $\Theta_I \approx 0.44$ ) consists of a hexagonal iodine overlayer compressed and rotated a few degrees from the R30° direction, giving rise to a long-range ( $\sim 20 \text{ \AA}$ ) corrugation in the STM image. The virtues of quantitative atomic-resolution STM for deducing such complex adlayer structures are pointed out.

\* Permanent address: Dept. of Chemistry, Purdue University, West Lafayette, Indiana 47907, USA

# Humboldt Senior Scientist, Fritz-Haber-Institut, 1992

The emergence of scanning tunnelling microscopy (STM) as an atomic-resolution probe of interfacial structure is exerting an increasingly major impact in surface science. While such STM studies have involved primarily surfaces in ultrahigh vacuum (UHV) environments, it has recently been demonstrated that the technique can yield information of comparably high quality at ordered solid-liquid interfaces, including systems under electrode-potential control [1-6]. Attention has been focussed so far on reconstruction of ordered low-index surfaces [4,5] and adlayer structures of simple atomic and molecular adsorbates [1,3,6]

A fundamental issue that arises in electrochemical as well as UHV surface science is the nature of adlayer structures as a function of adsorbate coverage. In the former case, coverage variations can often conveniently be induced by altering the electrode potential. Interesting benchmark systems in this regard are provided by halides adsorbed on noble metals. Iodide, in particular, exhibits very strong yet potential-dependent adsorption on gold surfaces to yield covalently bound iodine adatoms, as discerned readily by conventional methods such as differential capacitance-potential [7] and quartz crystal microbalance [8] measurements. While such techniques can yield adsorbate coverages and other thermodynamic parameters, they provide essentially no adlayer structural information.

We report here detailed adlayer structures for iodine on Au(111) in organic polar solvents and in air by means of STM, in comparison with structures also observed by STM for iodide adsorption in aqueous solution under electrode-potential control [9]. Comparisons are also made with adlayer structures observed recently by low-energy electron diffraction (LEED) following emersion from aqueous iodide solutions under potential control [10], and for iodine dosed onto Au(111) in UHV, also by LEED [11]. The present results illustrate the potential of STM to elucidate even complex non-commensurate adlayer structures in some detail.

The STM experiments in Berlin were performed with a "beetle"-type instrument (Delta-Phi-Electronic Co.) [12] in the constant-current mode. Some procedural details are given in ref.4. Mechanically polished iridium tips were used to image the iodine adlayers on Au(111) in air after transfer from the dosing solution. Results were obtained in

DTIC  
COPY  
INSPECT

☒  
☐  
☐

Code  
/or

A-1

diethylene glycol (DEG) or glycerol by placing a drop of the liquid onto the Au(111) surface (see ref.4). The Au(111) surfaces were prepared by evaporating an approximately 2000 Å thick gold film at  $10^{-6}$  torr onto quartz which was precoated with a 20 Å chromium layer to improve adhesion. The surfaces were pretreated immediately prior to the experiment by flame annealing at about 1000 K for 1 minute and then cooled in methanol. The iodine adlayers were formed either by including 10 mM iodine in the methanol solvent used for cooling, or by dipping the surface in a 10 mM iodine solution in methanol after cooling. In some cases 10 mM sodium iodide was used, with similar results.

Additional STM experiments were performed in aqueous solution under electrode potential control at Purdue University, using a Nanoscope II instrument (Digital, Inc.). Experimental details of the electrochemical STM have been given previously [13]. The tips were 0.01 in tungsten wire etched electrochemically in 1M KOH. These STM images were also obtained in the constant-current mode. The Au(111) surface was an oriented single crystal, prepared in LEI-CNRS Meudon, France, by Dr. A. Hamelin. It was also flame annealed, but cooled in ultrapure water.

At least two distinctly different types of iodine adlayer structures were commonly obtained on Au(111), either in air or in organic solvents. A typical STM image of the first, lower coverage, structure is shown in Fig. 1A. At first sight, the observed hexagon-like pattern is suggestive of the  $(\sqrt{3} \times \sqrt{3}) R 30^\circ$  structure (iodine coverage  $\Theta_I = 0.33$ ), common for such systems. Closer inspection, however, reveals the presence of significant distortions from an ideal hexagonal structure. While the row of spots running towards the top right-hand corner (row I) are separated by a distance  $d_{I-I} = 4.9 \pm 0.1$  Å, close to that (5.0 Å) expected for iodine atoms in the  $(\sqrt{3} \times \sqrt{3})$  structure, the  $d_{I-I}$  values for the remaining two rows (II and III) are significantly shorter,  $4.2 \pm 0.1$  Å. As a consequence, the angles between rows II and III with respect to I deviate by about  $5^\circ$  from that,  $60^\circ$ , characteristic of the threefold symmetric  $(\sqrt{3} \times \sqrt{3})$  structure. Essentially the same structural pattern was observed consistently on Au(111) both in air and in organic liquids.

Given the degree of thermal drift common in atom-resolution STM experiments, such apparently minor deviations from threefold

symmetry might be considered to be artifactual in origin. A valuable characteristic of the "beetle"-type STM, however, is the remarkably small degree of x-y distortion that routinely can be achieved. Moreover, the desired registry between the iodine adlattice and the underlying substrate could be discerned directly, since atomic-resolution images of the latter could reproducibly be obtained in the presence of the former by decreasing the resistance of the tunnelling gap by a factor of 10 - 20, thereby diminishing the tip-substrate distance. Figure 1B shows an example of such a substrate image, obtained immediately following the iodine adlattice image in Fig. 1A on the same surface domain. The presence of a symmetric hexagonal pattern is evident in Fig. 1B, the angles between the atomic rows being  $60 \pm 1^\circ$  with the interatomic distance,  $2.85 \pm 0.2 \text{ \AA}$ , close to that,  $d_{\text{Au-Au}} = 2.88 \text{ \AA}$ , expected for Au(111). Aligning the patterns in Figs. 1A and B shows that only row I of the iodine adlattice lies accurately along the  $R 30^\circ$  direction (i.e. bisecting the Au strings), rows II and III each rotated by about  $5^\circ$ . Significantly, the iodine adlayer pattern matches accurately the  $(5 \times \sqrt{3})$  structure proposed for the Au(111)-I system on the basis of LEED measurements [10]. This differs from the symmetric  $(\sqrt{3} \times \sqrt{3})$  pattern in that two of the three iodine rows are compressed yielding a higher coverage,  $\Theta_I = 0.4$ , with the iodine atoms occupying binding sites varying between twofold and threefold geometry. Perhaps surprisingly, however, no corresponding Z-corrugation is discernable in the STM images.

The other higher-coverage adlayer structural pattern observed in these experiments yields markedly different STM images. This is exemplified by the large-scale image shown in Fig. 2, obtained in diethylene glycol. A hexagonal pattern of iodine atoms is observed; unlike the  $(5 \times \sqrt{3})$  structure the angles between the rows are close to (within  $1\text{-}2^\circ$  of) the threefold symmetrical  $60^\circ$  value. A less symmetric aspect of these images, however, is the longer-range hexagonal corrugation pattern clearly discerned in Fig. 2. The distance between the groups of iodine atoms, forming periodic tunneling maxima, is  $19 \pm 0.5 \text{ \AA}$ . In addition, the directions of these longer-range corrugations are rotated by about  $9^\circ$  from the iodine rows. A further asymmetric property of this adlayer structure is that the iodine rows are also rotated slightly yet significantly, typically by  $4^\circ$ , in the

opposite direction with respect to the gold substrate  $R30^\circ$  direction. This angular relationship between the gold and iodine atomic rows was deduced similarly to the findings for the  $(5 \times \sqrt{3})$  structure by a direct comparison of the adlattice with the substrate STM image, whereby the latter was imaged by increasing markedly the tunneling current.

Careful examination of a number of images of this corrugated structure revealed that the  $d_{I-I}$  values ( $4.35 \pm 0.1 \text{ \AA}$  each), corresponding to an iodine coverage of about 0.44, are significantly different from those of the  $(5 \times \sqrt{3})$  structure. The observed longer-range corrugations, having a height of  $0.18 \pm 0.03 \text{ \AA}$ , presumably arise from periodic variations in the iodine binding site necessitated by the non-commensurate nature of the close-packed iodine and gold substrate lattices. Most probably, the tunnelling maxima (higher Z-values) are associated with iodine bound in atop (or near-atop) binding sites rather than nestled in the threefold hollow or bridging geometries normally preferred by such adsorbates. [Such higher Z-values for atop coordination are anticipated on simple geometric grounds, and indeed are very noticeable in the Pt(111)-I system [14,15]] Despite the complexity and non-unique nature of the unit cell, these pieces of information enable ball models for the high-coverage structure to be constructed. A likely model is depicted in Fig. 3; it features a longer-range periodicity of  $20 \text{ \AA}$ , close to the observed values, with a presumed uniform  $d_{I-I}$  value of  $4.4 \text{ \AA}$  and with the hexagonal iodine adlattice rotated clockwise by  $3^\circ$  from the  $R30^\circ$  substrate direction.

In the coverage range between 0.4 [( $5 \times \sqrt{3}$ ) phase] and 0.44 ("high coverage" phase), intermediate structures having local  $(5 \times \sqrt{3})$  symmetry, but featuring sharp corrugations which interrupt (and jog) the iodine rows, could be observed. An example of such a structure, corresponding to a coverage of 0.42, is shown in Fig. 2c.

Having deduced in some detail the nature of the iodine adlayers, observed in air or in organic liquids, as noted above it is of interest to relate them to the potential-dependent structures obtained in conventional electrochemical environments. To this end, in-situ STM measurements were undertaken at the Au(111)-aqueous interface, specifically in 0.1 M  $\text{HClO}_4$  containing 0.01-1 mM sodium iodide. A more detailed account, including the consequences of iodide electrooxidation, will be available elsewhere [9]. Briefly, at the most negative

potentials,  $E \approx -0.4$  to  $-0.1$  V vs. the saturated calomel electrode (SCE), the  $(\sqrt{3} \times \sqrt{3}) R 30^\circ$  iodine structure ( $\Theta_I = 0.33$ ) can be obtained. Evidence for this is provided by the  $d_{I-I}$  values,  $5.0 \pm 0.2$  Å, measured as before from the separation in the hexagonal arrays of spots, together with the  $30 \pm 2^\circ$  rotation of the iodine adlattice with respect to the Au(111) substrate. The latter was evaluated from the images obtained prior to iodide addition, at potentials positive of ca.  $-0.2$  V vs. SCE where the  $(1 \times 1)$  substrate structure is obtained [5b]. Similar STM images, showing apparently the  $(\sqrt{3} \times \sqrt{3})$  structure, could also readily be obtained after transfer to air (cf ref. 16). For  $E \geq -0.2$  V vs. SCE, careful examination of the in-situ STM images indicated the increasingly predominant formation of  $(5 \times \sqrt{3})$  domains ( $\Theta_I = 0.4$ ), as evidenced by a significant decrease of  $d_{I-I}$  in two of the three iodine rows. Since STM images obtained using the Nanoscope II are apparently more susceptible to distortions from thermal drift, however, the 20-25 % decrease in  $d_{I-I}$  and corresponding alterations in row direction were not so accurately evaluated as with the Besocke instrument.

For  $E \geq 0.3$  V vs. SCE, the  $(5 \times \sqrt{3})$  structure gives way increasingly to the higher-coverage corrugated patterns discussed above. A typical in-situ STM image of this structure is shown in Fig. 4. Similarly to the results described above (e.g. Fig. 3), the direction of the longer-range corrugation is rotated significantly (typically  $8 - 10^\circ$ ) from the iodine row direction, which in turn are rotated oppositely by a few degrees from the  $R 30^\circ$  substrate directions. It is therefore evident that essentially the same coverage-dependent adlayer structures, at least for  $\Theta_I \geq 0.4$ , are formed in the Au(111)-aqueous electrochemical environment as on Au(111) in air or in organic liquids. The potential-dependent appearance of the  $(\sqrt{3} \times \sqrt{3})$  and  $(5 \times \sqrt{3})$  adlattices observed by STM is also closely compatible with the electrode emersion-LEED results reported in ref. 10, although these authors did not identify the high-coverage incommensurate structure observed here.

Some additional comments are in order here regarding the anticipated relationship between iodine adlayers formed in such controlled-potential electrochemical systems and in other liquid (or gas-phase) environments. The charge state of the iodine adlayer will

not be affected in the former case if iodide rather than iodine is employed for solution dosing, since the adsorption thermodynamics are determined by the electrode potential. Nevertheless, the use of iodine, in particular, at gold-liquid interfaces *not* under external potential control would be expected to yield especially high iodine coverages on this basis. The reason is to be found in the value of the standard potential of the iodide-iodine redox couple,  $E^\circ \approx 0.5 \text{ V}$  vs. SCE in aqueous media. If the oxidized form of the redox couple, i.e. iodine, is used in this manner, the electrode potential will be pinned at values in the vicinity of  $E^\circ$ , or above. On the basis of the electrochemical STM data, high-coverage iodine adlayers should be prevalent under these conditions, in harmony with the findings described here.

In summary, the present STM results demonstrate the considerable potential of this technique to elucidate complex adlayer structures for ordered metal surfaces in air, liquid, as well as electrochemical and UHV environments. As such, then, the technique offers the intriguing prospect of contributing not only to structural elucidation at these fundamentally related, yet disparately treated, interfaces, but also to encourage the development of a more unified understanding of their behavior.

### Acknowledgements

M.J.W. is grateful to the Humboldt Foundation for a Senior Scientist Award. This work is supported in part by the Deutsche Forschungsgemeinschaft through Sfb 6 (J.K.S.) and by the U.S. Office of Naval Research (M.J.W.).



## References

- [1] O. M. Magnussen, J. Hotlos, R. J. Nichols, D. M. Kolb and R. J. Behm, Phys. Rev. Lett., 64 (1990) 2929.
- [2] S. L. Yau, C. M. Vitus and B. C. Schardt, J. Am. Chem. Soc., 112 (1990) 3677.
- [3] S. L. Yau, X. Gao, S. C. Chang, B. C. Schardt and M. J. Weaver, J. Am. Chem. Soc., 113 (1991) 6049.
- [4] W. Haiss, D. Lackey, J. K. Sass and K. H. Besocke, J. Chem. Phys., 95 (1991) 2193.
- [5] (a) X. Gao, A. Hamelin and M. J. Weaver, Phys. Rev. Lett., 67 (1991) 618,  
(b) X. Gao, A. Hamelin and M. J. Weaver, J. Chem. Phys., 95 (1991) 6993,  
(c) X. Gao, A. Hamelin, and M. J. Weaver, Phys. Rev. B 44 (1991) 10983.
- [6] T. Hachiya, H. Honbo, and K. Itaya, J. Electroanal. Chem., 315 (1991) 275.
- [7] A. Hamelin and J. P. Bellier, Surface Science, 78 (1978) 157.
- [8] M. R. Deakin, T. T. Li and O. R. Melroy, J. Electroanal. Chem., 243 (1988) 343.
- [9] X. Gao and M. J. Weaver, submitted to J. Am. Chem. Soc.
- [10] B. G. Bravo, S. L. Michelhaugh, M. P. Soriaga, I. Villegas, D. W. Suggs and J. L. Stickney, J. Phys. Chem., 95 (1991) 5245.
- [11] S. A. Cochran and H. H. Farrell, Surface Science, 359 (1980).
- [12] K. H. Besocke, Surface Science 181 (1987) 145.
- [13] C. M. Vitus, S-C. Chang, B. C. Schardt and M. J. Weaver, J. Phys. Chem., 95, (1991) 7559.
- [14] B. C. Schardt, S-L. Yau and F. Rinaldi, Science, 243 (1989) 150.
- [15] S-C. Chang, S-L. Yau, B. C. Schardt and M. J. Weaver, J. Phys. Chem., 95 (1991) 4787.
- [16] R. L. McCarley and A. J. Bard, J. Phys. Chem., 95 (1991) 9618.

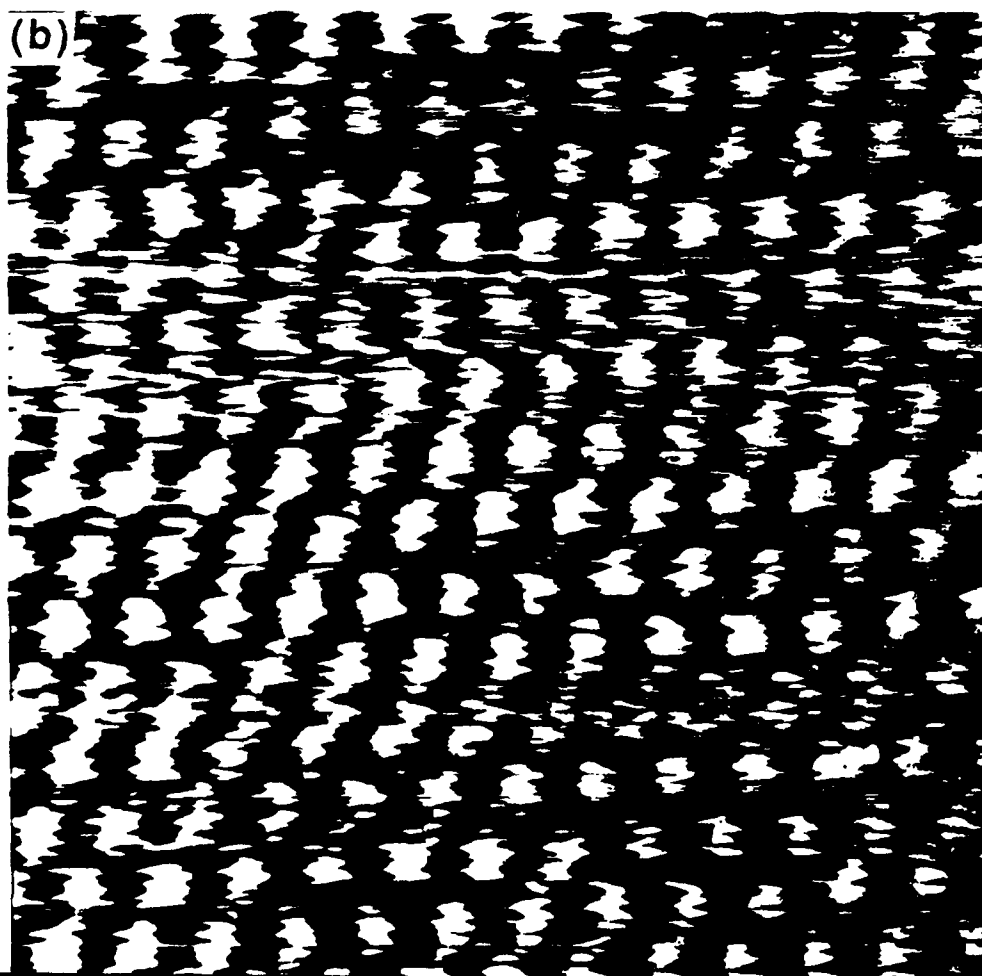
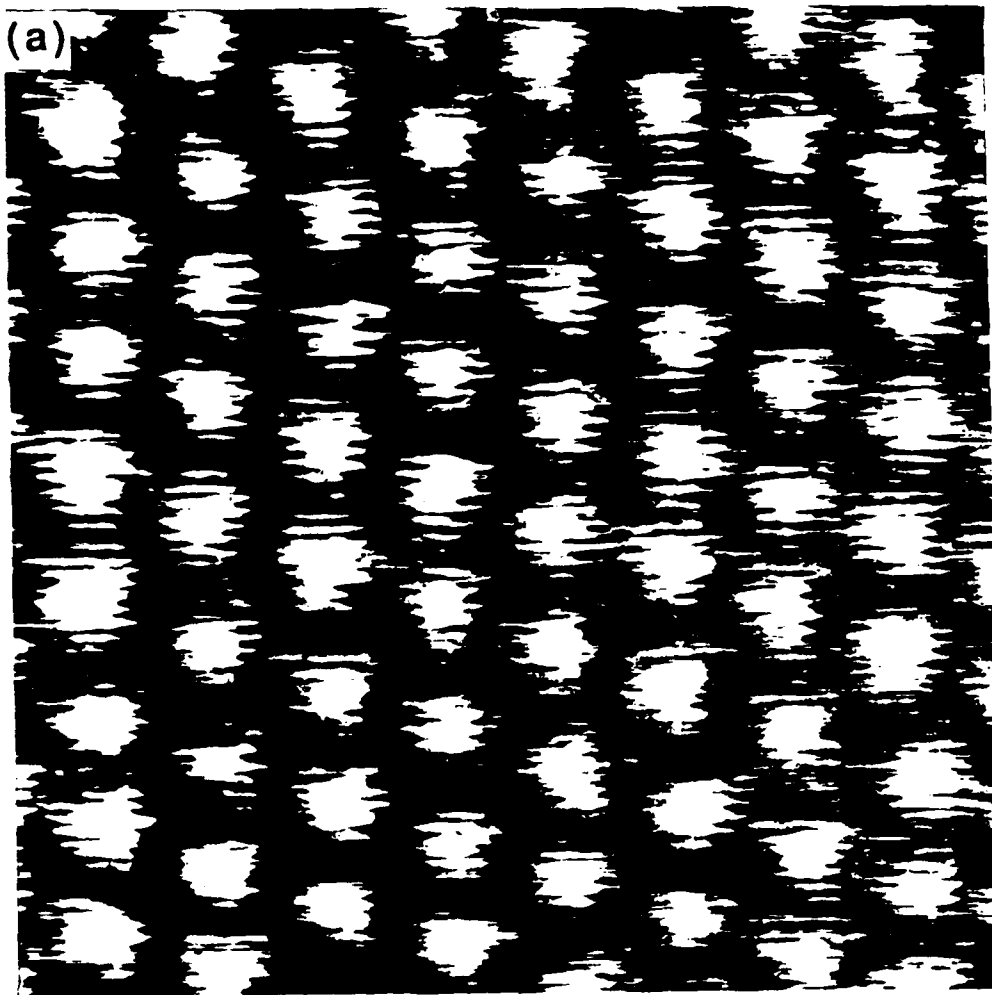
## Figure captions

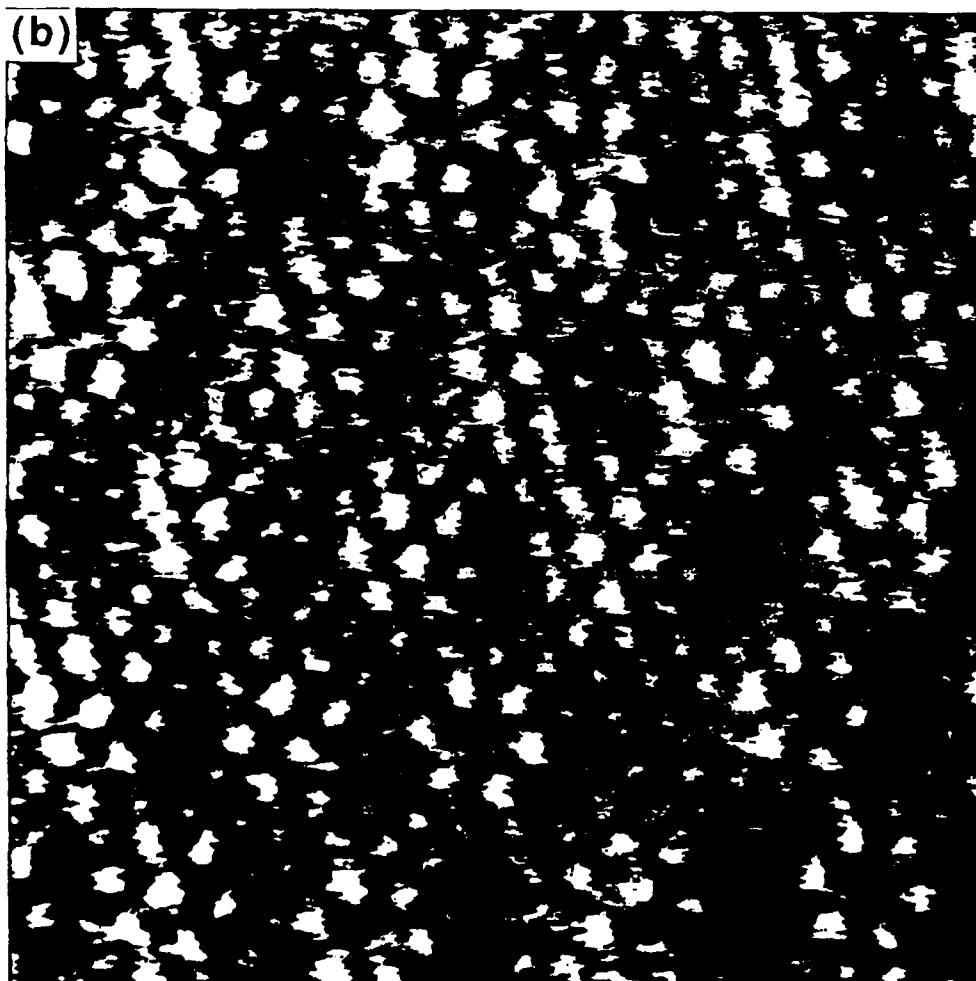
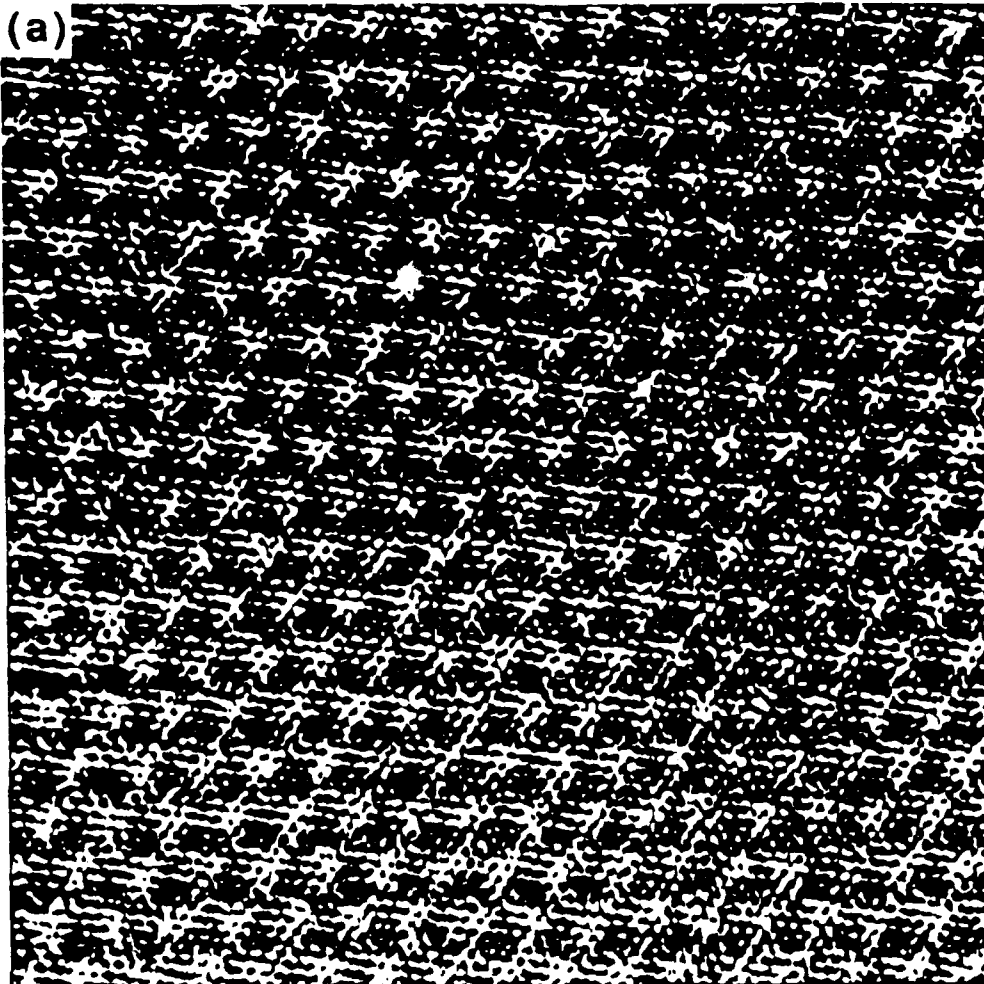
FIG.1. Atomic resolution STM images, taken in air, of the same  $35 \times 35 \text{ \AA}^2$  region of a gold film at different tunnel resistances showing (a) the  $(5 \times \sqrt{3})$  iodine structure ( $\Theta_I = 0.40$ ) on Au(111) at high tunnel resistance:  $V_t = 20 \text{ mV}$ ;  $I_t = 0.5 \text{ nA}$ . (b) the underlying unreconstructed Au(111) surface:  $V_t = 10 \text{ mV}$ ;  $I_t = 30 \text{ nA}$ .

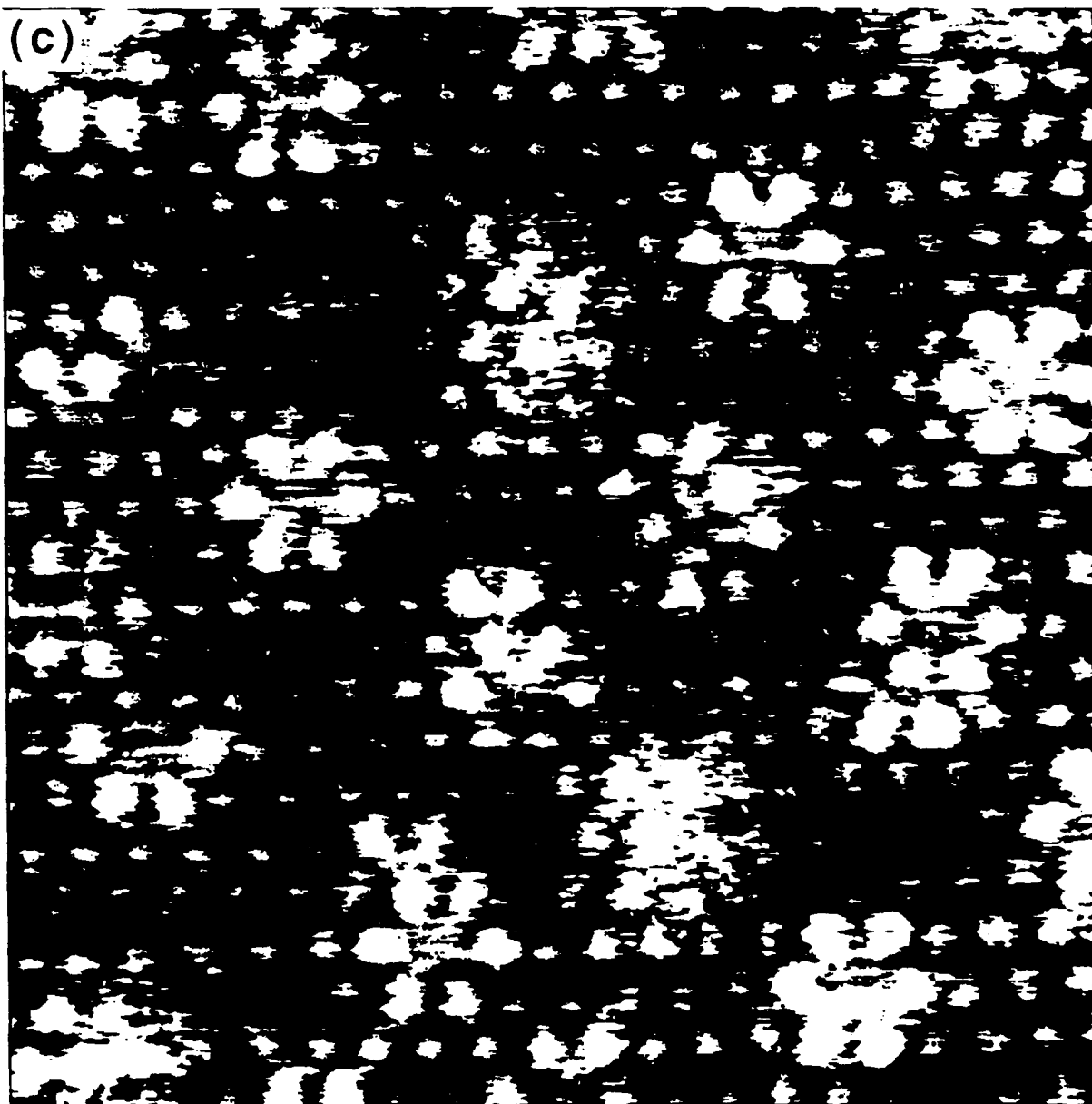
FIG.2. Atomic resolution images of iodine overlayers on Au(111). (a) large scale image ( $340 \times 340 \text{ \AA}^2$ ) taken in diethylene glycol of the high coverage iodine phase ( $\Theta_I = 0.44$ ) showing a long range hexagonal corrugation with a height of  $0.18 \text{ \AA}$  and a periodicity of  $20 \text{ \AA}$  superimposed on the atomic corrugation of the iodine atoms:  $V_t = -300 \text{ mV}$ ;  $I_t = 2.5 \text{ nA}$ . (b) STM image ( $85 \times 85 \text{ \AA}^2$ ) taken in air showing atomic details of the structure described in Figure 2(a):  $V_t = 100 \text{ mV}$ ;  $I_t = 20 \text{ nA}$ . (c) STM image ( $85 \times 85 \text{ \AA}^2$ ) taken in diethylene glycol corresponding to a coverage ( $\Theta_I = 0.42$ ), between the high coverage phase and the  $(5 \times \sqrt{3})$  structure, showing local disruption of the long range corrugation:  $V_t = 50 \text{ mV}$ ;  $I_t = 30 \text{ nA}$ .

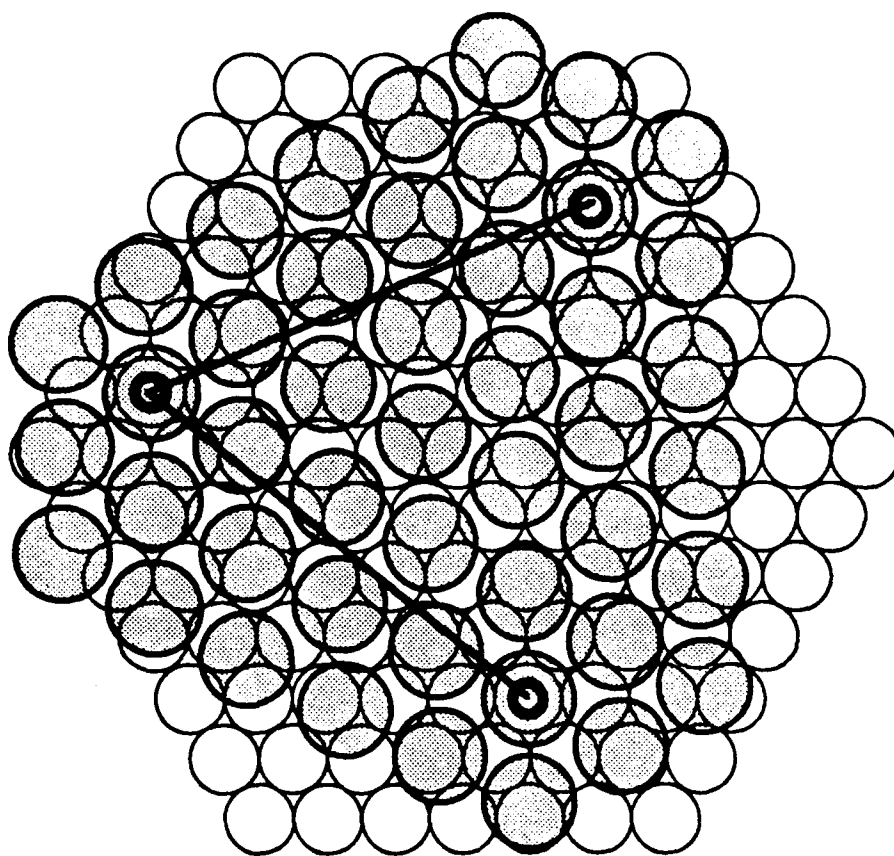
FIG.3. Ball model of the high-coverage iodine adlayer structure shown in Figs 2b and 4. Lines indicate one half of the unit cell; the inner circles denote iodine atoms in symmetry atop sites, corresponding to brightest spots in the STM image.

FIG.4. Fourier filtered in-situ STM image of the high-coverage I adlayer on Au(111) in  $0.1 \text{ M HClO}_4 + 1 \text{ mM NaI}$  at  $0.3 \text{ V vs SCE}$ ;  $V_t = -200 \text{ mV}$ ,  $I_t = 15 \text{ nA}$









Au(111)-I (7x7)R21.8°

